Article

A Deep Learning Model for Predicting the Laminar Burning Velocity of NH₃/H₂/Air

Wanying Yue, Bin Zhang *, Siqi Zhang, Boqiao Wang, Yuanchen Xia and Zhuohui Liang

Marine Engineering College, Dalian Maritime University, Dalian 116085, China; yuewanying@dlmu.edu.cn (W.Y.); zsq199812@163.com (S.Z.); wbqqbw717@dlmu.edu.cn (B.W.); xyc_0121@dlmu.edu.cn (Y.X.); lzh01112@dlmu.edu.cn (Z.L.)
* Correspondence: zb_2010@dlmu.edu.cn

Abstract: Both NH_3 and H_2 are considered to be carbon-free fuels, and their mixed combustion has excellent performance. Considering the laminar burning velocity as a key characteristic of fuels, accurately predicting the laminar burning velocity of $NH_3/H_2/Air$ is crucial for its combustion applications. The study made improvements to the XGBoost model and developed $\underline{N}H_3/\underline{H}_2/Air$ $\underline{L}aminar$ $\underline{B}urning$ $\underline{V}elocity$ $\underline{Net}$ (NHLBVNet), which adopts a composite hierarchical structure to connect the functions of feature extraction, feature combination, and model prediction. The dataset consists of 487 sets of experimental data after the exclusion of outliers. The correlation coefficient ($R^2 > 0.99$) of NHLBVNet is higher than that of the XGBoost model ($R^2 > 0.93$). Robustness experiment results indicate that this model can obtain more accurate prediction results than other models even under small sample datasets.

Keywords: laminar burning velocity (LBV); deep learning; $NH_3/H_2/Air$; XGBoost; predicting method

1. Introduction

In recent years, the increasing world population and rapid economic development have led to severe energy and environmental security risks, such as fossil fuel depletion and greenhouse gas emissions. Throughout the world, energy for a wide array of human and industrial endeavors has predominantly been derived from combustion processes. However, merely improving the performance level of combustion machinery to achieve low-emission goals cannot eliminate the current huge energy demand. Consequently, employing combustion processes with alternative, non-carbon-based fuels is seen as a high-impact auxiliary strategy for achieving greenhouse gas reduction targets [1,2].

Ammonia emerges as a pivotal energy vector, having promise across various sectors for carbon-neutral fuel storage, transit, and electricity generation. The carbon-free compound presents several benefits, notably its zero-carbon characteristic, elevated energy concentration, and the advantage of an existing industrial base for its creation [3]. However, compared to fossil fuels, ammonia fuel faces challenges, such as lower laminar flame speed [4], higher ignition energy, and NO_x emissions [5]. To overcome these obstacles, ammonia can be co-fired with hydrogen [6,7]. Qualitatively, the combustion of a mixture composed of ammonia and hydrogen can enhance the rate of smooth flame propagation and reduce the minimum ignition energy [8,9]. Ammonia-hydrogen combustion has tremendous development potential and prospects. Figure 1 shows the number of publications on ammonia-hydrogen combustion in recent years with data sourced from the Web of Science; thus, this paper's research on predicting the laminar velocity of ammonia-hydrogen has significant importance.

The laminar burning velocity (LBV) is a fundamental and crucial characteristic of fuel combustion, which provides an indication of the overall reactivity of the fuel, plays a critical role in the estimation of the thermal energy emission rate, and verifies both detailed and reduced combustion reaction mechanisms. Currently, the main methods for measuring

LBV include the Spherical Flame (SF), Constant Pressure Combustion Chamber (CPCC), Particle Tracking Velocimetry (PTV), Cylindrical Bomb (CB), Conical Flame (CF), and Heat Flux Burner (HFB) methods [10].
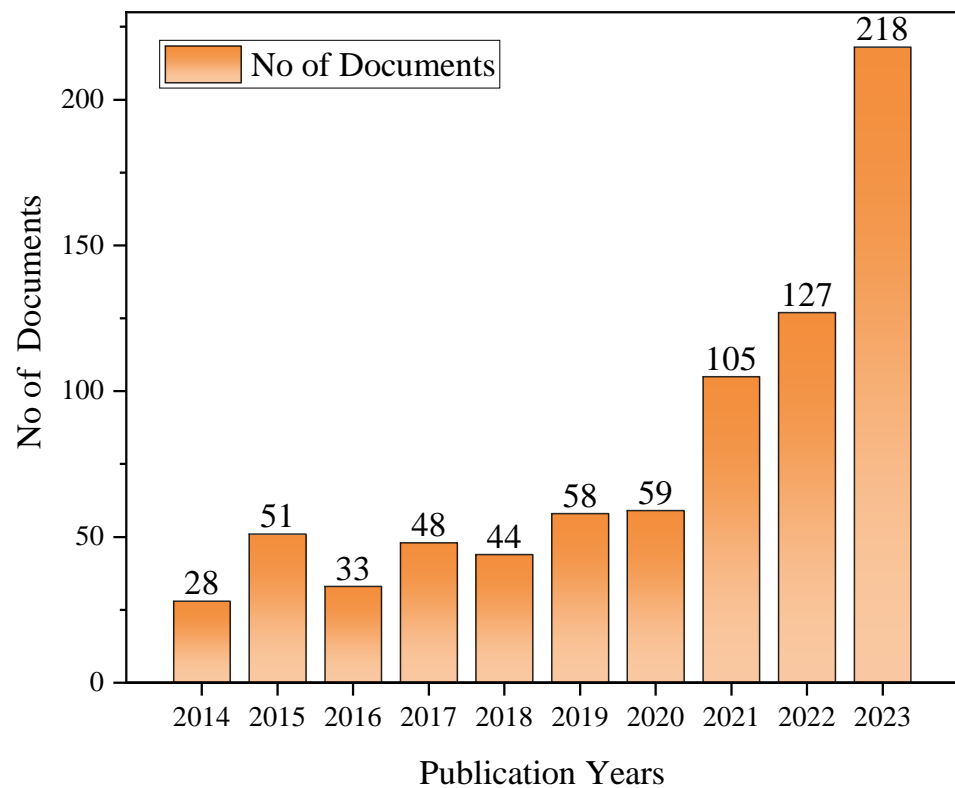

Figure 1. The number of recent publications on ammonia-hydrogen combustion research.

LBV can only be measured experimentally at low pressure and temperature, and the traditional experimental methods for deriving LBV under different conditions for various fuels are very cumbersome. Nevertheless, despite their limitations, the experimental measurements of LBV continue to serve as a primary benchmark for verifying the accuracy of different fuel combustion mechanisms [11,12].

An alternative approach for determining LBV involves employing computational tools like Cantera, Chemkin, and OpenSMOKE++, which utilize chemical kinetics mechanisms to calculate LBV using one-dimensional simulation methods. In the realm of engine simulation, applying comprehensive combustion models to both zero-dimensional (0D) and one-dimensional (1D) models presents significant computational challenges and is often deemed impractical due to the high demand on processing power. Machine learning approaches can be leveraged to expedite the computation of LBV within both 0D and 1D engine simulation models, without compromising the accuracy of the results [13].

Machine learning methods have been applied to predict the laminar burning velocity and to study the dependence of LBV on various factors. Some studies have used Support Vector Machine (SVM) and Artificial Neural Network (ANN) methods to compare the prediction of LBV for low-carbon fuels, with results indicating that ANN methods performs better with single fuels, while the opposite is true for mixed fuels [14]. Zhongyu Wan [15] selected a squared exponential Gaussian Process Regression (GPR) model for predicting the laminar burning speed of single hydrocarbons and oxygenated fuels. Cihat Emre Üstün [16], by comparing different ML models, recommended using GPR and Neural Network (NN) algorithms to predict the LBV of $NH_3/H_2/Air$. Gadi Udaybhanu [17] integrated artificial neural networks (ANNs) with Genetic Algorithms (GAs), employing a GA-ANN model to predict the LBV of isooctane blended with various fuels. In addition, Yanqing Cui [18]

established a BP-GA model for the ignition delay prediction of an n-butane/hydrogen mixture to obtain better prediction ability.

However, the studies undertaken still have their limitations. Due to the limited experimental values of LBV and the small sample size, the literature reviewed incorporates a significant amount of data generated by simulation software such as Chemkin 4.1 into the datasets. The accuracy of these simulated data depends on the values of the reaction rate constants, reaction orders, and activation energies within different chemical kinetics mechanisms, which may still have some discrepancies compared to experimental data. Current methods are unable to achieve good prediction results from the small-scale experimental datasets obtained after removing simulated data, which limits the accuracy of the models under real experimental conditions. The research dataset is solely sourced from publicly accessible experimental data, thereby enhancing the precision of the study.

This study proposes an innovative model based on XGBoost for predicting the LBV of ammonia and hydrogen, named NHLBVNet, which demonstrates excellent performance on small-scale datasets. Additionally, the model introduces a combustion feature module and a combustion prediction module, further enhancing the model's interpretability and highlighting the superiority of NHLBVNet over other baseline models. The code for the NHLBVNet model has been placed on GitHub (https://github.com/master032/NHLBVNet (accessed on 17 September 2024)).

2. Methods
2.1. The NHLBVNet Model
2.1.1. Model Architecture

The NHLBVNet model is structured to include a combustion feature module and a separate combustion prediction module, with the model structure illustrated in Figure 2. In this paper, the combustion feature module operates to extract relevant data and to formulate characteristics from the vector of the combustion reaction information vector h_i, resulting in a combustion feature vector q_i. The combustion feature vector q_i is then input into the feature prediction module to obtain the model's predicted laminar burning velocity result vector s_i.
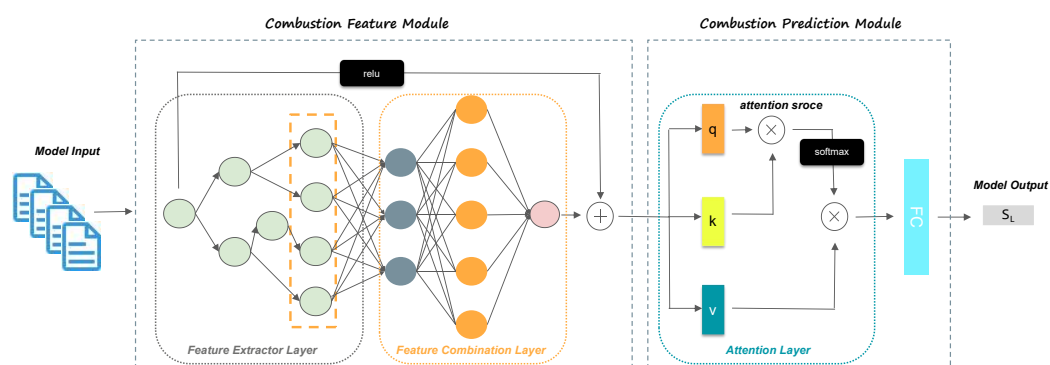

Figure 2. Structure of the NHLBVNet Model.

Different from other LBV prediction models, NHLBVNet incorporates a multi-layer structure in its design, which facilitates the model's thorough learning of the data distribution. The model is segmented into multiple modules, enhancing its scalability. Additionally, the adoption of the ResNet architecture effectively mitigates information loss within the model.

2.1.2. Model Input

This study employs the dataset derived from Section 3.1 for both model training and prediction. Through the organization of the data, this paper has established datasets that include a pressure information dataset P, temperature information dataset T, a hydrogen blending ratio information dataset X, and an equivalence ratio information dataset K.

The combustion reaction information dataset H is used as the input for the model, wherein combustion reaction information vectors h_i are employed to represent the specific data from combustion experiments, where $h_i \in R^{|H| \times 5}$ and $|H|$ denote the number of entries in the combustion reaction information dataset H. Each combustion reaction information vector h_i is composed of the aforementioned four types of information, where $h_i = p_i, t_i, x_i, k_i$ and $p_i \in P, t_i \in T, x_i \in X, k_i \in K$.

2.1.3. Combustion Feature Module

The task of the combustion feature module is to thoroughly extract features from the input data, thereby providing support for the combustion prediction module to output precise results. The combustion feature module initially employs XGBoost [19] for preliminary feature extraction.

XGBoost is an algorithm based on gradient boosting decision trees [20,21]. Gradient boosting involves predicting the residuals or errors from previous models and then summing these to form the final prediction. It is referred to as gradient boosting because it employs the gradient descent algorithm [22,23] to minimize the loss when introducing new models into the ensemble. XGBoost also enhances the interpretability of the model [24]. Compared to random forests, XGBoost is faster and more accurate, offering superior model performance. A significant amount of work has utilized XGBoost for tasks of feature selection and feature combination [25–27].

Within the combustion feature module, the formula used for XGBoost is represented as Equation (1).

$$y_i = \sum_{k=1}^{M} f_k(h_i) \tag{1}$$

where h_i represents the combustion reaction information obtained from the ith experiment; XGBoost learns a base learner f_k for each feature, and then sums the outputs of all base learners as the predicted laminar burning velocity of the ammonia-hydrogen mixture, thereby conducting gradient boosting training.

To further extract features, the combustion feature module employs a multi-layer perceptron [28] for preliminary feature learning of the data. As a classic machine learning method, the multi-layer perceptron is capable of fitting tasks while minimizing the loss of information [29]. Through the multi-layer perceptron, the model can obtain the combustion feature embedding vectors. The formula used in this stage is shown as Equation (2).

$$e_i = Wh_i + b \tag{2}$$

where e_i represents the combustion feature embedding vector obtained from the ith experiment; W represents the weight matrix; and b denotes the bias term.

Subsequently, the combustion feature module employs a structure akin to residual neural networks [30] for information integration. Given the value of the data within the dataset, to enhance the model's capacity for learning the distribution of the original data, this research adds the outputs from the various base learners $f_k(h_i)$ in XGBoost to the combustion reaction information h_i obtained from the ith experiment. This approach strengthens the model's learning of the raw data. The formula used is shown as Equation (3).

$$q_i = \alpha \circ f_k(h_i) + (1 - \alpha) \circ h_i \tag{3}$$

where α is a hyperparameter used to control the proportion of various data within the ResNet structure; f_k represents the decision tree obtained from the kth training iteration, with each $f_k(h_i)$ corresponding to an independent tree structure, where each $f_k(h_i)$ scores the sample h_i. These scores are collected; the obtained scores are multiplied by the hyperparameter α and added to the combustion reaction information to obtain the ith combustion feature vector q_i.

After processing through the combustion feature module, the model conducts comprehensive feature learning and integration of the combustion reaction information h_i. The resulting combustion feature vector q_i will then be passed as the output of the combustion feature module to the subsequent module.

2.1.4. Combustion Prediction Module

The combustion prediction module is utilized for predicting the laminar burning velocity, and this module consists of an attention layer and an output layer. The attention mechanism directs focused attention to key information, thereby conserving computational resources and rapidly acquiring the most pertinent information [31,32].

In order to screen the obtained combustion feature embedding vector e_i, the combustion feature vectors q_i from the previous module are collected to form the dataset of combustion feature vectors Q_f, which is then placed into an attention module. The combustion prediction module employs an attention mechanism to score the features that affect the laminar burning velocity of ammonia-hydrogen mixtures, thereby highlighting the impact of significant features on the model's predictive outcomes. This utilizes the attention mechanism to assign weights that further emphasize the core combustion data. The attention function formula used within the module is presented as Equation (4).

$$
\begin{aligned}
Q &= W_Q Q_f \\
K &= W_K Q_f \\
V &= W_V Q_f \\
\text{Attention}(Q, K, V) &= \text{softmax}\left(\frac{QK^T}{\sqrt{d_k}}\right)V
\end{aligned}
\tag{4}
$$

where $a_i \in A$ represents the attention score of the combustion feature vector; W_Q, W_K, and W_V denote the matrix of parameters required for computing the attention scores; d_k is the length of the combustion feature vector; the attention score a_i for the combustion feature vector q_i is assigned by calculating the similarity between the combustion feature vector q_i obtained from the ith experiment and the combustion feature vector q_j obtained from the jth experiment.

The softmax function is frequently used as an activation function to achieve the effect of reducing model linearization and normalizing model results. In this paper, the softmax function is used with the computational formula (5) as follows:

$$
y_k = \frac{\exp(a_k)}{\sum_{i=1}^{n} \exp(a_i)}
\tag{5}
$$

where exp refers to the exponential function, and a_i is the input to the function.

Finally, the combustion prediction module employs a linear layer as the output layer to adjust the final predicted LBV for ammonia-hydrogen mixtures. The formula used is as shown in Equation (6).

$$
\begin{aligned}
x_i &= a_i * q_i \\
s_i &= softmax(W_5 x_i + b_3) + b_4
\end{aligned}
\tag{6}
$$

where softmax is the activation function; W_5 is the matrix of parameters required for the calculation; b_3 and b_4 are the bias parameters needed for the output layer computation. This module multiplies the attention scores a_i obtained from the combustion feature module for the combustion feature embedding vectors q_i to derive the combustion reaction vectors x_i. The combustion reaction vectors x_i are then input into the linear layer to yield the model's predicted result vector s_i.

2.2. Model Training

The task of this paper is a prediction task, leveraging the NHLBVNet model to forecast the LBV of ammonia-hydrogen mixtures based on provided datasets of the pressure information dataset P, temperature information dataset T, hydrogen blending ratio information dataset X, and equivalence ratio information dataset K. In this paper, to comprehensively consider the model's predictive accuracy under single conditions and the distribution gap of the model's overall output, the model employs a composite loss function of the Root Mean Square Error (RMSE) and the Mean Absolute Error (MAE) to measure the prediction accuracy [33] of the model.

- Root Mean Square Error
  The root mean square error (RMSE) is calculated based on the Mean Squared Error (MSE) by taking the square root of its output. It measures the prediction gap by computing the sample standard deviation of the differences (referred to as residuals) between the predicted values and the observed values, with the RMSE indicating the degree of dispersion of the samples. In regression tasks, a smaller RMSE indicates that the distribution of the prediction results is closer to the distribution of the actual data. The formula for RMSE used in this paper is shown as Equation (7).

$$RMSE(X, h) = \sqrt{\frac{1}{m} \sum_{i=1}^{m} (h(x_i) - y_i)^2} \tag{7}$$

- Mean Absolute Error
  The mean absolute error (MAE) measures the prediction gap by calculating the mean of the absolute discrepancies between the forecasted and actual values. MAE is a linear score where all individual discrepancies have equal weight in the average, and compared to the root mean square error (RMS0.E), it imposes less penalty on higher discrepancies. The formula for MAE used in this paper is shown as Equation (8).

$$MAE(X, h) = \frac{1}{m} \sum_{i=1}^{m} |h(x_i) - y_i| \tag{8}$$

- Loss Function
  In the NHLBVNet model, a composite formula using both the mean absolute error (MAE) and the root mean square error (RMSE) is employed to simultaneously measure the absolute error and the distribution gap of the predicted values, thereby enhancing the model training effectiveness. A threshold value, denoted as λ, is set to limit the impact of the MAE and RMSE on the overall loss. The loss function utilized in this study is presented in Equation (9).

$$L = \lambda MAE + (1 - \lambda)RMSE \tag{9}$$

3. Results and Discussion

3.1. Dataset

This study involved the collection of experimental data on ammonia-hydrogen combustion from multiple papers and organized it into a unified dataset format for model training and prediction. A comprehensive collection of 553 datasets pertaining to the stratified combustion of $NH_3/H_2/Air$ mixtures was gathered under a wide range of experimental settings (hydrogen content X_{H_2}, temperature T, pressure P, and equivalence ratio φ). Table 1 presents the sources of the collected data and the details of the dataset used in this paper.

Table 1. Experimental data on LBV from academic sources.

Author(s)	Year	X_{H_2}	φ	T (K)	P (MPa)	LBV (cm/s)
Han et al. [34]	2019	0.025–0.4	0.7–1.6	298	0.1–0.5	6.0–33.90
Wang et al. [35]	2020	0.4–0.6	0.6–1.6	298–493	0.05–0.2	8.85–64.98
Lhuillier et al. [36]	2020	0.05–0.6	0.8–1.4	298	0.1–0.7	4.81–140.21
Shrestsha et al. [37]	2021	0.05–0.3	0.8–1.4	298–423	0.05–0.15	7.38–50.01
Gotama et al. [38]	2022	0.1–0.4	0.8–1.8	298–443	0.1	9.44–38.75
Zhou et al. [39]	2022	0.1–0.7	0.7–1.4	298–423	0.1	5.56–30.28

To illustrate the differences between these datasets, we conducted a significance analysis on the dataset used in this article. The Kolmogorov–Smirnov test was used to calculate the correlation between the same variable in different datasets. The significance scores of all variables between the two tables were averaged to obtain a significance matrix. The significance test results are shown in Figure 3.
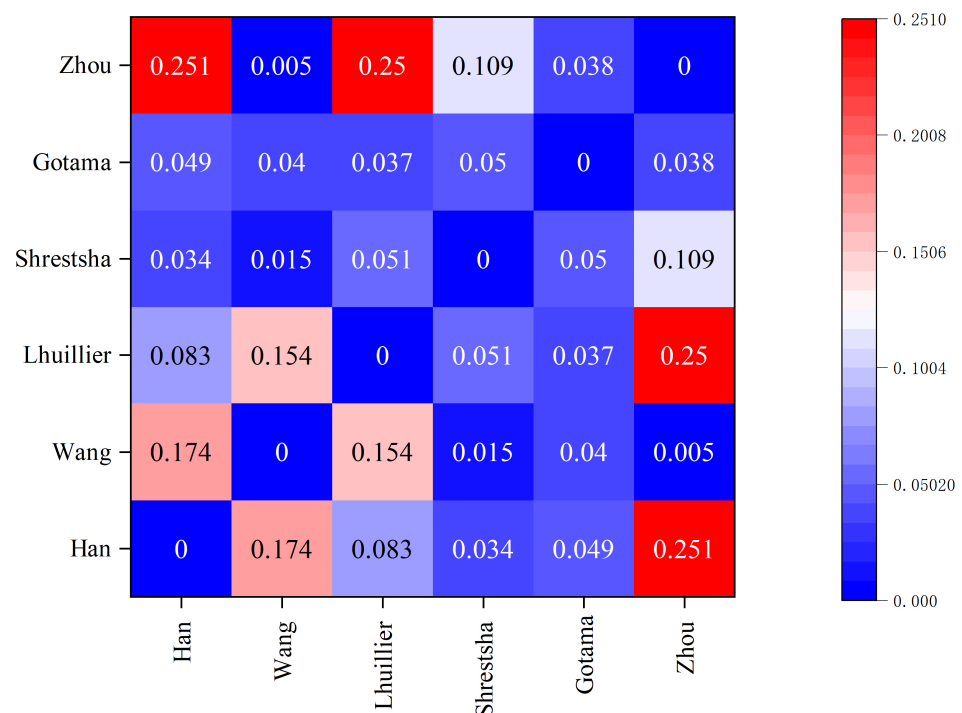
Figure 3. Significance testing between different datasets.

When the *p*-value is less than 0.05, the two tables reach 95% significance. From the matrix, it can be seen that most of the datasets used in the article have significant correlations. This also indicates that using experimental data from different authors for model training is feasible, with errors within an acceptable range.

3.2. Data Analysis and Processing

During combustion experiments, the dataset may encounter outliers due to experimental apparatus inaccuracies or human operational errors. Such data points deviate from the general distribution pattern of the dataset.

Experimental data that include outliers can impact the model training; therefore, this research processed the aforementioned data and conducted outlier removal. Since the four factors cannot be considered simultaneously, the dataset is grouped by different T, P, X_{H_2}, and φ, and outliers are screened out for each group.

Our screening method involves fixing three conditions to obtain a scatter plot of a specific condition versus LBV and calculating the 95% confidence interval, as shown in Figure 4, which shows the relationship between φ and LBV at P = 1 atm, T = 298 K,

X_{H_2} = 0.3. Samples that fall outside this confidence interval are considered outliers and are removed. The blue area represents the 95% confidence interval for the dataset in this group, and the red data points are the excluded outliers.
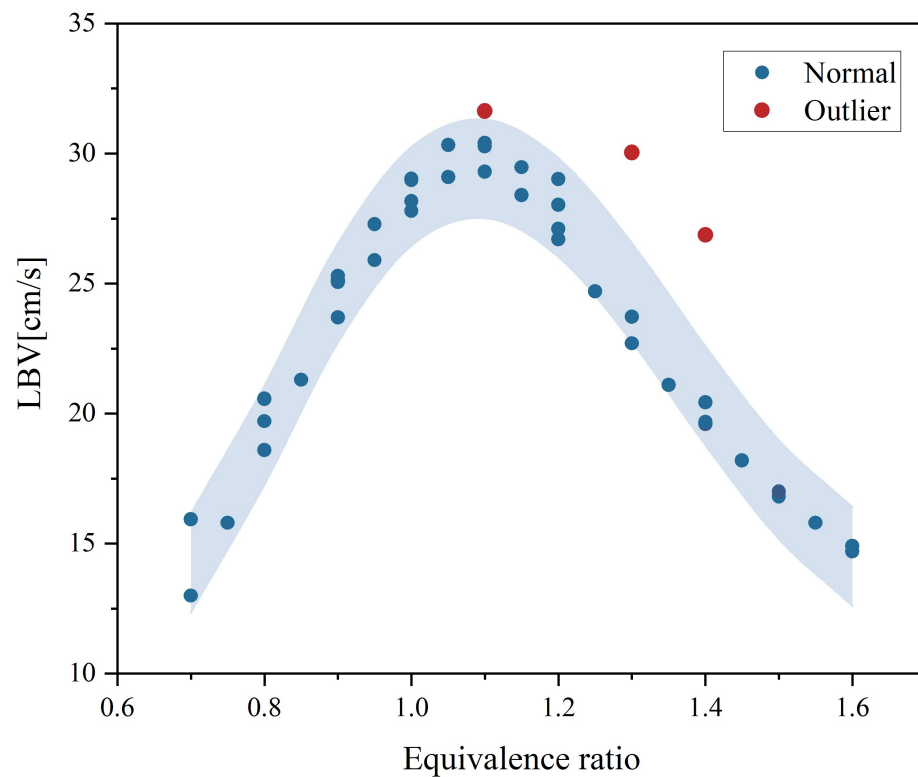

Figure 4. Outlier screening in the group with P = 1 atm, T = 298 K, X_{H_2} = 0.3.

Using this method, 67 sets of outlier data were eliminated, leaving 486 sets of data. The excluded outliers will not appear in the dataset of the model and will not participate in the training, evaluation, and analysis of the model. Table 2 delineates the spectrum of collected experimental observations and enumerates the remaining datasets following the exclusion of outliers.

The structured dataset was partitioned into segments for training, testing, and validation purposes, with a distribution ratio of 7:1.5:1.5, as shown in Table 3. We use training and testing sets for model training and parameter selection, and validation sets for model result validation. By using this dataset partitioning method, it is possible to avoid overfitting of the model due to incomplete evaluation of the model.

Table 2. The ranges of the dataset parameters used by NHLBVNet.

Parameters	Values
Pressure	1–7 bar
Temperature	298–493 K
Hydrogen fuel fraction	0.025–0.6
Equivalence ratio	0.6–1.8
LBV	4.81–140.21 cm/s
No. of exp. points	486

This study meticulously examines the relationship between four key factors (hydrogen content X_{H_2}, temperature T, pressure P, and equivalence ratio φ) to uncover the underlying characteristics of the dataset involved. The findings, as depicted in Figure 5, reveal that X_{H_2} has a substantial impact on LBV, indicating its importance as a primary driver in

the experimental data. Temperature's impact ranks as the second most substantial factor, suggesting that thermal conditions must be closely monitored to maintain optimal LBV.

Table 3. Details of data partitioning.

Dataset	Proportion
Train Dataset	70%
Test Dataset	15%
Verification Dataset	15%

In Figure 5, we also conducted a significance analysis, where the more asterisks present indicate a more significant correlation between the feature variables. From the analysis results, it can be observed that a majority of the variables in the dataset exhibit significance, while a minority show strong significance.

While the pressure and equivalence ratio also play a role, their effects are less pronounced compared to X_{H_2} and temperature. This suggests that, although they should not be disregarded, they may not require the same level of meticulous control as the other two factors. Moreover, the correlations among these factors are found to be weak, indicating a degree of independence that can be exploited for individual optimization without causing significant disruptions to the other variables. This nuanced understanding of the factors at play provides a solid foundation for further research and practical applications aimed at enhancing LBV.
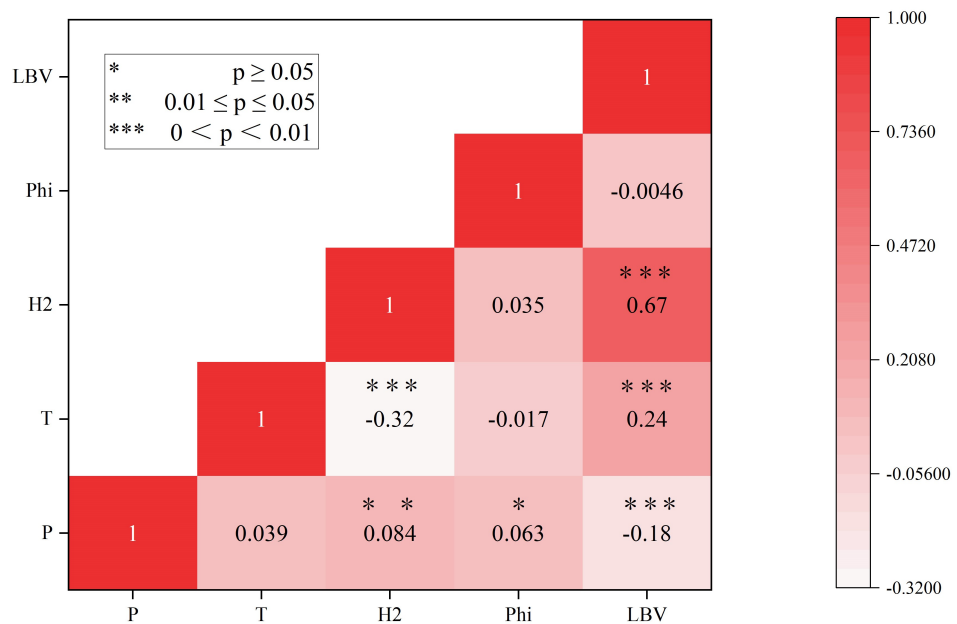

Figure 5. Correlation heatmap of the dataset.

3.3. Results Analysis

The NHLBVNet model proposed in this study is based on an improvement of XGBoost, achieving $R^2 > 0.99$. A comparison of its prediction results with those of XGBoost is shown in Figure 6. It is evident that the XGBoost predictions of LBV have a significant error in the range of 20–60 cm/s, even exceeding 25% error. In contrast, NHLBVNet addresses this issue, providing accurate predictions within the 20–60 cm/s range, with errors generally less than 10%.
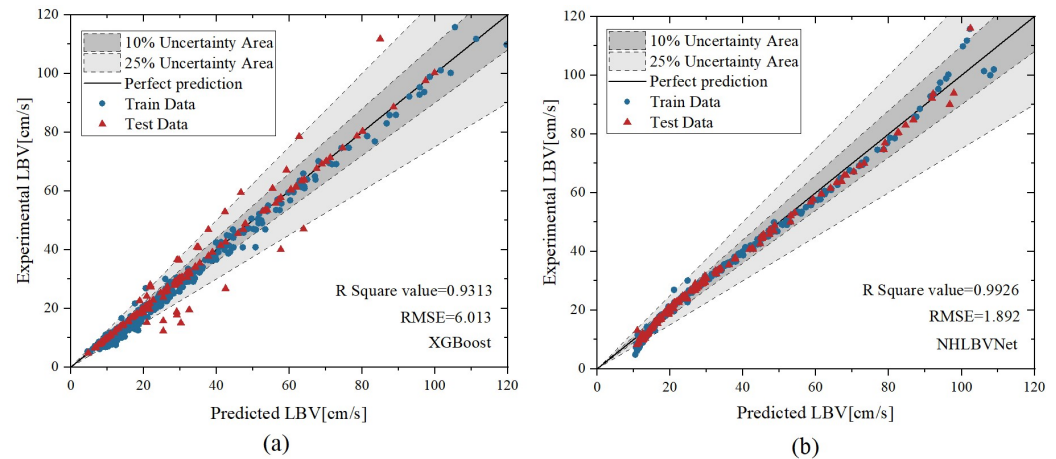
Figure 6. (**a**) XGBoost and (**b**) NHLBVNet prediction results.

This paper also selects MLP (Multi-Layer Perceptron), LR (Logistic Regression), XG-Boost, and XGBoost+MLP as baseline models for comparison, with the results shown in Table 4. The multi-layer perceptron (MLP) is characterized as a feedforward type of artificial neural network, which encompasses an input layer, an output layer, and a series of intermediary layers known as hidden layers. The MLP compared in this paper is a basic three-layer perceptron. Due to its limited model capacity, it did not achieve good results across the three metrics. Logistic regression stands out as a prevalent linear statistical model that is often employed for a variety of tasks, and its results are better than those of MLP. XGBoost is an optimization and improvement of the Gradient Boosting Decision Tree (GBDT) algorithm and has achieved excellent results in regression tasks.

Table 4. The best performance comparison on dataset.

Model	R^2	MAE	RMSE
MLP	0.766	19.326	7.934
LR	0.783	18.151	7.011
XGBoost	0.931	6.013	2.812
XGBoost + MLP	0.956	3.838	1.959
NHLBVNet	**0.993**	**1.892**	**1.225**

In the experiments, XGBoost was the best-performing model among all the baseline models, achieving good results. XGBoost + MLP adds a multi-layer perceptron layer after the output of XGBoost to further learn the data distribution, and its performance is further enhanced based on XGBoost.

In summary, the NHLBVNet model results in multi-layer improvements to XGBoost and enhances the prediction accuracy of LBV of $NH_3/H_2/Air$. It outperforms current mainstream methods in both R^2 and MSE as well as MAE metrics. The results indicate that the NHLBVNet model provides more accurate predictions of the LBV for ammonia-hydrogen mixtures.

3.4. Ablation Study

To ascertain the contribution of individual elements within the NHLBVNet architecture introduced herein, the following ablation experiments were designed:

- NHLBVNet—ResNet
  In the NHLBVNet model, the ResNet structure is eliminated, which means that in the combustion feature extraction module, the output of the linear layer is directly used as the output of the combustion feature extraction module.
- NHLBVNet—FCL

The feature combination layer in the NHLBVNet model is eliminated, no longer performing the collection and combination of features, and instead, the output from the feature extractor layer serves directly as the output for the combustion feature module.

- NHLBVNet—Attention Layer (Att)

  The attention structure in the NHLBVNet model is eliminated, and attention weights are no longer assigned and calculated for features; all features are considered equally important for model learning.

The results of the ablation experiments for the corresponding modules are listed in Table 5. When the respective structures are removed, the model performance is affected to varying degrees, which validates the necessity of each module for NHLBVNet.

Table 5. Comparison of ablation experiment results.

Model	R^2	MAE	RMSE
NHLBVNet-ResNet	0.979	2.603	1.711
NHLBVNet-FCL	0.988	2.167	1.509
NHLBVNet-Att	0.983	2.214	1.568
NHLBVNet	**0.993**	**1.892**	**1.225**

3.5. Parameter Analysis

To investigate the influence of model parameters on the NHLBVNet model's performance, this section describes parameter experiments on XGBoost, XGBoost + MLP, and the NHLBVNet model.

In the NHLBVNet model, both the feature combination layer and the output layer utilize a multi-layer perceptron (MLP) for prediction, where the neuron count in each layer is also a pivotal model parameter. This section first investigates the neuron count within the feature combination layer and the output layer in the NHLBVNet. The experimental findings are presented in Figure 7.
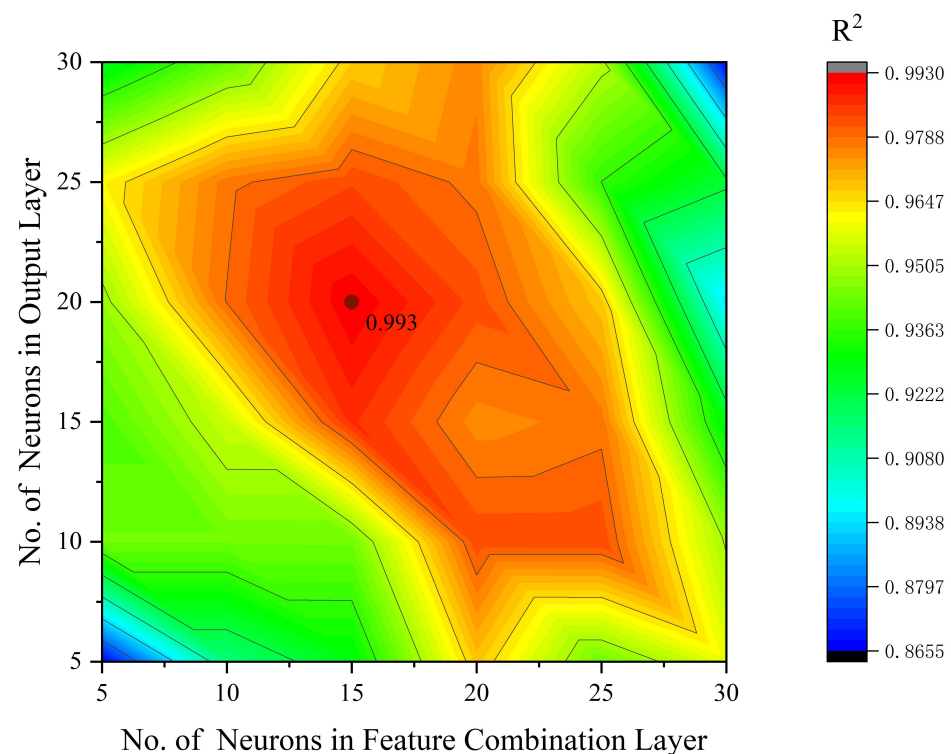

Figure 7. Results of the number of neurons experiment.

In this experiment, the performance of the model is evaluated by monitoring the R^2 similarity coefficient. It can be noted that when there is a smaller neuron count across

each layer, the model exhibits a larger error, indicating a poorer fit and a more significant deviation in the distribution of the output data. On the other hand, increasing the number of neurons to a greater extent leads to overfitting, which is characterized by a sudden drop in the R^2 similarity coefficient. This suggests that there is an optimal range for the number of neurons that balances between underfitting (larger error due to poor model complexity) and overfitting (reduced performance due to excessive complexity). Based on the parameter experimentation, this paper sets the neuron count in the output layer to 20 and in the feature combination layer to 15, which yields the most precise outcomes for the model.

This section then explores the effect of training epochs on the model, with the performance of the models at different training epochs shown in Figure 8.
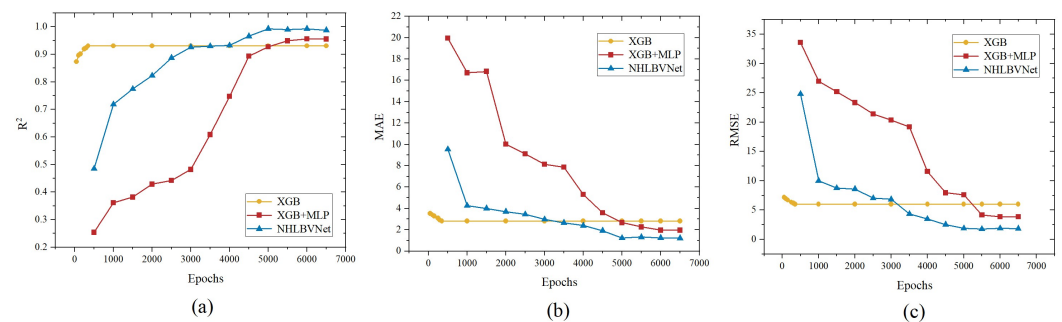

Figure 8. Training epochs experiment results (**a**) R^2; (**b**) MAE; (**c**) RMSE.

From Figure 8, it can be observed that XGBoost reaches stability with fewer training iterations. When the quantity of training epochs is insufficient, both the overall distribution and accuracy of the NHLBVNet model and XGBoost + MLP are inferior to XGBoost. With an escalating count of training iterations, the performance of the NHLBVNet model and XGBoost + MLP gradually surpasses that of XGBoost, with the NHLBVNet model showing the best performance. The results of the parameter experiments indicate that when the training epochs exceed 4000, the performance of the NHLBVNet model surpasses all baseline models. Furthermore, when the training epochs are around 5000, the NHLBVNet model can perform optimally and become stable.

3.6. Robustness Analysis

The results analysis of this paper found that the NHLBVNet model outperforms the baseline models on the small-scale dataset. To substantiate the NHLBVNet model's reliability and sturdiness concerning various datasets, this paper reports robustness experiments on XGBoost, XGBoost+MLP, and the NHLBVNet model.

The experimental setup was devised to incrementally diminish the training set's volume, all the while keeping the training parameters unchanged, thereby investigating the dependency of each model on the data. The size of the training set was controlled by adjusting the proportion it represents within the entire dataset, with models being tested at training set proportions of 70%, 60%, 50%, and 40%, while the test set remained fixed. The R^2 similarity coefficient was utilized as the evaluation metric to assess the overall accuracy of each model's output. The robustness experiment's findings are illustrated in Figure 9.
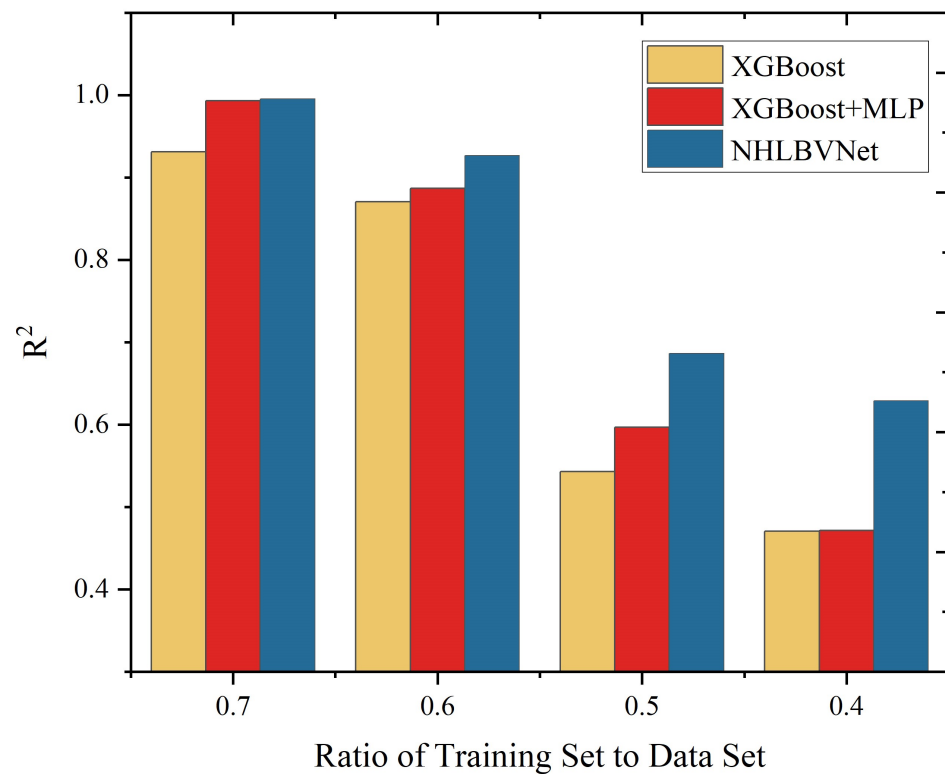
Figure 9. Results of the robustness analysis.

As the size of the training set decreased, the performance of all models showed a significant decline. Notably, the combined model of XGBoost + MLP experienced the most substantial decrease, while the NHLBVNet model exhibited the least reduction in overall accuracy. This indicates that compared to other baseline models, the NHLBVNet model is capable of delivering superior performance even with small-scale datasets. The NHLBVNet model outperformed the baseline models across various datasets, once again demonstrating the superiority and effectiveness of the NHLBVNet model.

3.7. Error Analysis

To explore the circumstances under which the model makes mistakes, this section conducts an error analysis. Specifically, this section tallies the mean residual errors predicted by the model, and the distribution is shown in Table 6.

Table 6. Residuals of the model across various intervals.

LBV Intervals	0–20	20–40	40–60	60–80	80–100	100–120	120–140
Avg Residuals	1.948	1.808	3.930	2.951	4.330	9.019	39.726

It can be observed that as LBV increases, the loss output by the model also gradually increases. To investigate this issue, we conducted further statistical analysis on the data, obtaining the proportion of data in each segment, as shown in Figure 10.

We found that when LBV is high, the amount of data is smaller, leading to a decline in the model's predictive performance. This is consistent with the characteristics of combustion experiments; when under high temperature and high pressure conditions, LBV is larger, but this also places more stringent demands on the experimental equipment, resulting in less available data, which, in turn, leads to a decrease in the model's predictive capability.
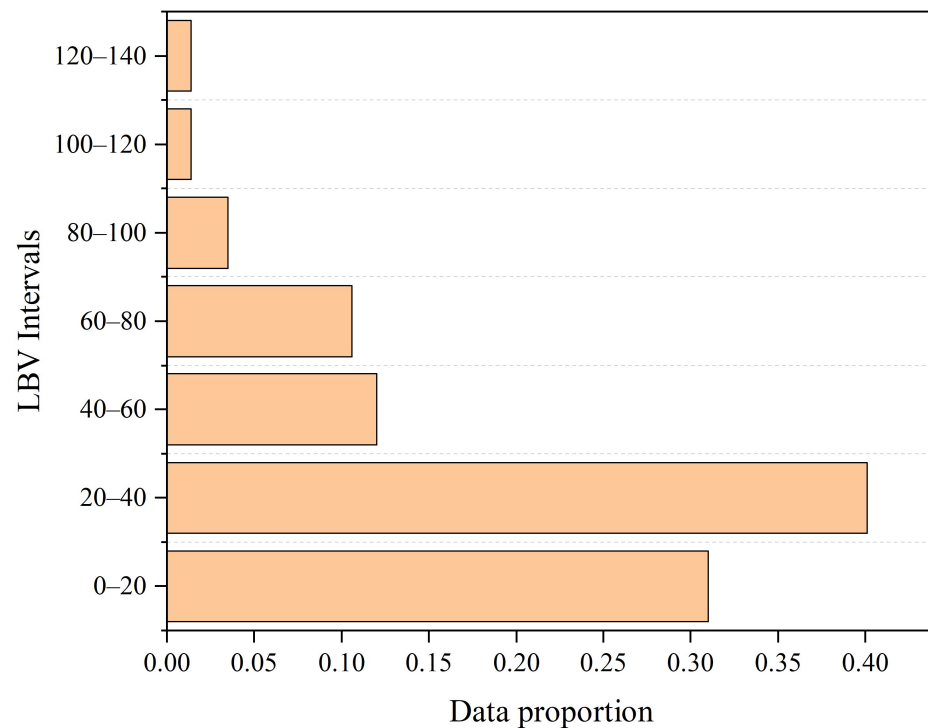
Figure 10. Data proportions by LBV segmentation.

4. Conclusions

This work has developed a new machine learning (ML) model to estimate the LBV of $NH_3/H_2/Air$, applicable across diverse conditions. Experimental data from various conditions were sourced from existing scholarly works and cleaned of outliers to form a dataset for ML training. The study concludes the following:

- In terms of prediction accuracy for the LBV of $NH_3/H_2/Air$, the NHLBVNet model proposed in this paper performs better ($R^2 > 99\%$) than the improved XGBoost model ($R^2 > 93\%$).
- The ablation experiment results of NHLBVNet are all higher than the XGBoost model, proving the effectiveness and necessity of each component of the NHLBVNet model.
- Robustness experiment results indicate that the NHLBVNet model outperforms other baseline models on small-scale datasets, showing better generalization capabilities.

Given these conclusions, the NHLBVNet model developed in this paper still maintains its superiority on small-sample datasets. It holds promise to replace the laborious experimental data acquisition or numerical simulation calculations for LBV, providing support for the exploration of $NH_3/H_2/Air$ combustion mechanisms.

Institutional Review Board Statement: Not applicable.

Informed Consent Statement: Not applicable.

Data Availability Statement: The data presented in this study are available on request from the corresponding author.

Conflicts of Interest: The authors declare no conflicts of interest.

References

1. Kobayashi, H.; Hayakawa, A.; Somarathne, K.K.A.; Okafor, E.C. Science and technology of ammonia combustion. *Proc. Combust. Inst.* **2019**, *37*, 109–133. [CrossRef]
2. Masoumi, S.; Ashjaee, M.; Houshfar, E. Laminar flame stability analysis of ammonia-methane and ammonia-hydrogen dual-fuel combustion. *Fuel* **2024**, *363*, 131041. [CrossRef]
3. Morlanés, N.; Katikaneni, S.P.; Paglieri, S.N.; Harale, A.; Solami, B.; Sarathy, S.M.; Gascon, J. A technological roadmap to the ammonia energy economy: Current state and missing technologies. *Chem. Eng. J.* **2021**, *408*, 127310. [CrossRef]
4. Lesmana, H.; Zhu, M.; Zhang, Z.; Gao, J.; Wu, J.; Zhang, D. Experimental and kinetic modelling studies of laminar flame speed in mixtures of partially dissociated NH_3 in air. *Fuel* **2020**, *278*, 118428. [CrossRef]
5. Hayakawa, A.; Arakawa, Y.; Mimoto, R.; Somarathne, K.K.A.; Kudo, T.; Kobayashi, H. Experimental investigation of stabilization and emission characteristics of ammonia/air premixed flames in a swirl combustor. *Int. J. Hydrogen Energy* **2017**, *42*, 14010–14018. [CrossRef]
6. Li, J.; Huang, H.; Kobayashi, N.; He, Z.; Nagai, Y. Study on using hydrogen and ammonia as fuels: Combustion characteristics and NOx formation. *Int. J. Energy Res.* **2014**, *38*, 1214–1223. [CrossRef]
7. Xiao, H.; Valera-Medina, A.; Bowen, P.J. Modeling combustion of ammonia/hydrogen fuel blends under gas turbine conditions. *Energy Fuels* **2017**, *31*, 8631–8642. [CrossRef]
8. Han, X.; Wang, Z.; He, Y.; Zhu, Y.; Cen, K. Experimental and kinetic modeling study of laminar burning velocities of NH_3/syngas/air premixed flames. *Combust. Flame* **2020**, *213*, 1–13. [CrossRef]
9. Li, H.; Xiao, H.; Sun, J. Laminar burning velocity, Markstein length, and cellular instability of spherically propagating NH_3/H_2/Air premixed flames at moderate pressures. *Combust. Flame* **2022**, *241*, 112079. [CrossRef]
10. Konnov, A.A.; Mohammad, A.; Kishore, V.R.; Kim, N.I.; Prathap, C.; Kumar, S. A comprehensive review of measurements and data analysis of laminar burning velocities for various fuel+ air mixtures. *Prog. Energy Combust. Sci.* **2018**, *68*, 197–267. [CrossRef]
11. Pichler, C.; Nilsson, E.J. Reduced kinetic mechanism for methanol combustion in spark-ignition engines. *Energy Fuels* **2018**, *32*, 12805–12813. [CrossRef]
12. Otomo, J.; Koshi, M.; Mitsumori, T.; Iwasaki, H.; Yamada, K. Chemical kinetic modeling of ammonia oxidation with improved reaction mechanism for ammonia/air and ammonia/hydrogen/air combustion. *Int. J. Hydrogen Energy* **2018**, *43*, 3004–3014. [CrossRef]
13. Pulga, L.; Bianchi, G.; Falfari, S.; Forte, C. A machine learning methodology for improving the accuracy of laminar flame simulations with reduced chemical kinetics mechanisms. *Combust. Flame* **2020**, *216*, 72–81. [CrossRef]
14. Shahpouri, S.; Norouzi, A.; Hayduk, C.; Fandakov, A.; Rezaei, R.; Koch, C.R.; Shahbakhti, M. Laminar flame speed modeling for low carbon fuels using methods of machine learning. *Fuel* **2023**, *333*, 126187. [CrossRef]
15. Wan, Z.; Wang, Q.D.; Wang, B.Y.; Liang, J. Development of machine learning models for the prediction of laminar flame speeds of hydrocarbon and oxygenated fuels. *Fuel Commun.* **2022**, *12*, 100071. [CrossRef]
16. Üstün, C.E.; Herfatmanesh, M.R.; Valera-Medina, A.; Paykani, A. Applying machine learning techniques to predict laminar burning velocity for ammonia/hydrogen/air mixtures. *Energy AI* **2023**, *13*, 100270. [CrossRef]
17. Udaybhanu, G.; Reddy, V.M. A hybrid GA-ANN and correlation approach to developing a laminar burning velocity prediction model for isooctane/blends-air mixtures. *Fuel* **2024**, *360*, 130594. [CrossRef]
18. Cui, Y.; Wang, Q.; Liu, H.; Zheng, Z.; Wang, H.; Yue, Z.; Yao, M. Development of the ignition delay prediction model of n-butane/hydrogen mixtures based on artificial neural network. *Energy AI* **2020**, *2*, 100033. [CrossRef]
19. Chen, T.; Guestrin, C. Xgboost: A scalable tree boosting system. In Proceedings of the 22nd ACM SIGKDD International Conference on Knowledge Discovery and Data Mining, San Francisco, CA, USA, 13–17 August 2016; pp. 785–794.
20. Lee, J.H.; Shin, J.; Realff, M.J. Machine learning: Overview of the recent progresses and implications for the process systems engineering field. *Comput. Chem. Eng.* **2018**, *114*, 111–121. [CrossRef]
21. Yuan, X.; Chen, F.; Xia, Z.; Zhuang, L.; Jiao, K.; Peng, Z.; Wang, B.; Bucknall, R.; Yearwood, K.; Hou, Z. A novel feature susceptibility approach for a PEMFC control system based on an improved XGBoost-Boruta algorithm. *Energy AI* **2023**, *12*, 100229. [CrossRef]
22. Ruder, S. An overview of gradient descent optimization algorithms. *arXiv* **2016**, arXiv:1609.04747.
23. Yang, B.; Liu, Y.; Liu, Z.; Zhu, Q.; Li, D. Classification of Rock Mass Quality in Underground Rock Engineering with Incomplete Data Using XGBoost Model and Zebra Optimization Algorithm. *Appl. Sci.* **2024**, *14*, 7074. [CrossRef]
24. Song, Z.; Cao, S.; Yang, H. An interpretable framework for modeling global Solar radiation using tree-based ensemble machine learning and Shapley additive explanations methods. *Appl. Energy* **2024**, *364*, 123238. [CrossRef]
25. Jiang, Z.; Che, J.; He, M.; Yuan, F. A CGRU multi-step wind speed forecasting model based on multi-label specific XGBoost feature selection and secondary decomposition. *Renew. Energy* **2023**, *25*, 802–827. [CrossRef]
26. Wang, W.; Xiong, W.; Wang, J.; Tao, L.; Li, S.; Yi, Y.; Zou, X.; Li, C. A user purchase behavior prediction method based on XGBoost. *Electronics* **2023**, *12*, 2047. [CrossRef]
27. Yao, S.; Kronenburg, A.; Stein, O. Efficient modeling of the filtered density function in turbulent sprays using ensemble learning. *Combust. Flame* **2022**, *237*, 111722. [CrossRef]

28. Alzubi, J.; Nayyar, A.; Kumar, A. Machine learning from theory to algorithms: An overview. *J. Physics Conf. Ser.* **2018**, *1142*, 012012. [CrossRef]

29. Hou, J.; Pan, H.; Guo, T.; Lee, I.; Kong, X.; Xia, F. Prediction methods and applications in the science of science: A survey. *Comput. Sci. Rev.* **2019**, *34*, 100197. [CrossRef]

30. He, K.; Zhang, X.; Ren, S.; Sun, J. Deep residual learning for image recognition. In Proceedings of the IEEE Conference on Computer Vision and Pattern Recognition, Las Vegas, NV, USA, 27–30 June 2016; pp. 770–778.

31. Niu, Z.; Zhong, G.; Yu, H. A review on the attention mechanism of deep learning. *Neurocomputing* **2021**, *452*, 48–62. [CrossRef]

32. Nie, T.; Yao, S.; Wang, D.; Wang, C.; Zhao, Y. MAPPNet: A Multi-Scale Attention Pyramid Pooling Network for Dental Calculus Segmentation. *Appl. Sci.* **2024**, *14*, 7273. [CrossRef]

33. Wang, Q.; Ma, Y.; Zhao, K.; Tian, Y. A comprehensive survey of loss functions in machine learning. *Ann. Data Sci.* **2020**, *9*, 187–212. [CrossRef]

34. Han, X.; Wang, Z.; Costa, M.; Sun, Z.; He, Y.; Cen, K. Experimental and kinetic modeling study of laminar burning velocities of NH_3/air, NH_3/H_2/air, NH_3/CO/air and NH_3/CH_4/air premixed flames. *Combust. Flame* **2019**, *206*, 214–226. [CrossRef]

35. Wang, S.; Wang, Z.; Elbaz, A.M.; Han, X.; He, Y.; Costa, M.; Konnov, A.A.; Roberts, W.L. Experimental study and kinetic analysis of the laminar burning velocity of NH_3/syngas/air, NH_3/CO/air and NH_3/H_2/air premixed flames at elevated pressures. *Combust. Flame* **2020**, *221*, 270–287. [CrossRef]

36. Lhuillier, C.; Brequigny, P.; Lamoureux, N.; Contino, F.; Mounaïm-Rousselle, C. Experimental investigation on laminar burning velocities of ammonia/hydrogen/air mixtures at elevated temperatures. *Fuel* **2020**, *263*, 116653. [CrossRef]

37. Shrestha, K.P.; Lhuillier, C.; Barbosa, A.A.; Brequigny, P.; Contino, F.; Mounaïm-Rousselle, C.; Seidel, L.; Mauss, F. An experimental and modeling study of ammonia with enriched oxygen content and ammonia/hydrogen laminar flame speed at elevated pressure and temperature. *Proc. Combust. Inst.* **2021**, *38*, 2163–2174. [CrossRef]

38. Gotama, G.J.; Hayakawa, A.; Okafor, E.C.; Kanoshima, R.; Hayashi, M.; Kudo, T.; Kobayashi, H. Measurement of the laminar burning velocity and kinetics study of the importance of the hydrogen recovery mechanism of ammonia/hydrogen/air premixed flames. *Combust. Flame* **2022**, *236*, 111753. [CrossRef]

39. Zhou, S.; Cui, B.; Yang, W.; Tan, H.; Wang, J.; Dai, H.; Li, L.; ur Rahman, Z.; Wang, X.; Deng, S.; et al. An experimental and kinetic modeling study on NH_3/air, NH_3/H_2/air, NH_3/CO/air, and NH_3/CH_4/air premixed laminar flames at elevated temperature. *Combust. Flame* **2023**, *248*, 112536. [CrossRef]